Available online at www.eccomasproceedia.org
Eccomas Proceedia COMPDYN (2023) 4575-4589

ECCOMAS
Proceedia

COMPDYN 2023
9th ECCOMAS Thematic Conference on
Computational Methods in Structural Dynamics and Earthquake Engineering
M. Papadrakakis, M. Fragiadakis (eds.)
Athens, Greece, 12-14 June 2023

CONTROL OF THE STRUCTURAL RESPONSE OF A HIGH-RISE BUILDING UNDER WIND LOAD USING A TUNED MASS DAMPER INERTER (TMDI)

Daniela Vallejo-Paniagua[1], Mariana Castro-Osorio[2], Verónica Valencia-Valencia[2], Luis A. Lara-Valencia[2], and John J. Blandón-Valencia[2].

[1] Universidad Nacional de Colombia sede Medellín
Carrera 80 N.º65-223, Núcleo Robledo. Medellín, Colombia.
dvallejo@unal.edu.co

[2] Universidad Nacional de Colombia sede Medellín
Carrera 80 N.º65-223, Núcleo Robledo. Medellín, Colombia.
{mcastroos, vvalenciav, lualarava, jjblandon}@unal.edu.co

Abstract

Several studies have been done on structural control over the last few decades, with the intent to reduce the structural response of buildings under environmental loads. Generally, the purpose of these works is to mitigate the accelerations and displacements that are generated and compromise the safety of people and the stability of the structure itself. To achieve the desired controlled behavior of the structure, a control device can be used. Among the different existing control alternatives, passive control devices have proven to be very effective and convenient for a structure because they use their own mass to generate inertial forces that counteract the external forces acting on the system. This paper explores the numerical design of a TMDI using a nature-like metaheuristic to find the optimal parameters of the device to implement it in a high-rise building under wind load. For this purpose, the grey wolf optimizer (GWO) is used to reduce the objective functions related to peak displacement and root mean square (RMS) value of acceleration. The results show an important improvement in the response of the building, meaning the displacements and accelerations were mitigated, proving that the TMDI is a suitable device for structural control.

Keywords: Structural control, tuned mass damper inerter, Grey Wolf Optimizer, wind load.

ISSN:2623-3347
Peer-review under responsibility of the organizing committee of COMPDYN 2023.
doi: 10.7712/120123.10742.20136

1 INTRODUCTION

The effort to reduce vibrations caused by seismic or wind loads in buildings is especially important, as these loads can result in significant displacements and acceleration forces on the structure, compromising its stability and putting the safety of its inhabitants at risk. Therefore, the implementation of control strategies to mitigate their effects is essential for ensuring the safety of the building and its users [1].

Several methods have been investigated to reduce the structural response under dynamic loads such as increasing the inertia of the structure by modifying its mass or stiffness. However, the use of control devices has been gaining more popularity for their effectiveness in a wide range of applications and the variety of available devices [2]. Some control devices, known as active devices, work by applying an external counterforce. Others, known as passive devices, use the properties of the structure and the device to generate forces that counteract external loads.

Passive control devices have been widely studied to mitigate vibrations benefiting from the fact that they do not need an external source of energy and they are able to generate great damping [3]. Passive devices such as Adding Damper and Stiffness (ADAS), Tuned Liquid Column Damper (TLCD), and Viscoelastic Dampers have been shown to effectively improve the response of structures under environmental loads [4–6]. Another passive device, which has been studied in numerous research is a tuned mass damper (TMD), a concept that was first proposed by Den Hartog [7] and consists of a mass, a spring, and a damper tuned to the fundamental frequency of the structure. It is typically placed on the top floor of a building, where it helps to mitigate the most severe response to wind or seismic loads [8, 9]. This is achieved by redirecting the vibrations of the structure to the device, where they are then dissipated through the damping [10]. However, its ability to reduce the response of buildings to wind and seismic loads is limited due to construction constraints to place a device of a large mass on the top floor. Therefore, the mass of the device is selected with a typical upper limit of 5% of the total mass of the structure being controlled [11].

As an improvement of a TMD, a tuned mass damper inerter (TMDI) was proposed by Marian and Giaralis [12]. The TMDI consists of a traditional TMD with an attached inerter device. An inerter is a mechanical device with two terminals that links the TMD with the previous level it is located on. The most favorable feature of the inerter is amplifying its own small mass, a characteristic that allows it to have a significant impact. Since the inerter was proposed by Smith [13] many studies have been done, concluding that it is an effective mechanism to enhance passive devices to mitigate the structural response of buildings [14–16].

Despite the similarities of both devices (TMD and TMDI), and the positive performance of the first, a TMDI becomes a better option to reduce displacements and accelerations generated by environmental loads because nowadays, structures tend to grow vertically and slimmer. Therefore, the mass needed by the device to work adequately in a high-rise building is greater than the one needed for lower structures. Furthermore, these kinds of structures need to undergo an analysis of the wind load effect which they are very susceptible to, due to their slenderness [17, 18]. Research on buildings exposed to wind vibrations using a TMDI has yielded promising results [19, 20].

The optimal design of a TMDI depends on the structure it is intended for, as the parameters that govern the device must be adjusted to match the fundamental frequency of the building [21]. To find these parameters, metaheuristics optimization algorithms have proven to be a reliable method to use while being simple and applicable to a wide range of problems [22, 23]. In a metaheuristic approach, a set of possible solutions is randomly generated, and a function is used to evaluate the quality of each solution. The best solutions are then used to generate new solutions through a

process of exploration. This process is repeated until a satisfactory solution is found or a stopping criterion is met.

In this work, the Grey Wolf Optimizer (GWO) will be used to obtain the parameters needed to optimally design the TMDI. GWO is a nature-inspired, metaheuristic algorithm that is used to optimize solutions to a problem [24, 25]. The algorithm is inspired by the hunting behavior of a pack of wolves and replicates the hierarchy and cooperation present in a wolf pack. GWO has been shown to be an effective optimization technique while considering the constraints and limitations of the problem.

This paper aims to develop a TMDI that can minimize the structural impact of wind on high-rise buildings, specifically reducing maximum displacements and acceleration. The device will be located on the top floor of a 37th -story building and the inerter will be attached one floor below it. Finally, the GWO will be used and is expected to provide an efficient optimization process to find the optimal parameters for the TMDI: the frequency and damping ratio. The use of a TMDI optimized with the GWO optimization technique provides a reliable and efficient means to reduce the dynamic response of a high-rise building, being able to reduce up to 37% of the displacements suffered during a wind gust. Overall, the TMDI system provides a promising approach to addressing the challenges posed by dynamic wind loads and can help to enhance the resilience and reliability of structures.

2 MATHEMATICAL MODEL OF A TUNED MASS DAMPER INERTER (TMDI) IN A MULTI-DEGREE OF FREEDOM BUILDING

The mathematical model is presented for a plane frame with *n*-degrees of freedom, related to the horizontal translation per level of the frame subjected to an external force.

2.1 The inerter

The inerter, as presented in Figure 1, is a small mechanical element with two terminals which main characteristic is that the relative acceleration that the device experience at the terminals is also proportional to the applied force on them, in this case, the dynamic load. The internal force (F_b) resisting in each terminal can be written as shown in equation (1):

$$F_b = b(\ddot{u}_2 - \ddot{u}_1) \tag{1}$$

Where $\ddot{u}_1$ y $\ddot{u}_2$ are the accelerations on terminals 1 and 2, respectively, and *b* is the inerter proportionality constant that defines the device.

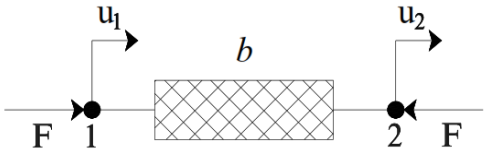

Figure 1: Outline of an inerter device.

An inerter can enhance the performance of passive control devices such as a TMD. TMDs have been successful in reducing building vibrations, however, their efficacy is restricted by the amount

of mass that can be located on the top floor. This not only reduces the inertial force that the device can produce but also restricts its impact to only one frequency since the mass of the device is fixed. This becomes increasingly difficult as buildings become taller. The inerter, on the other hand, is installed on the top floor and adds a minimal amount of mass while providing a resisting force of up to 200 times the added mass [26].

2.2 Equation of motion for an *n* degree of freedom system equipped with a TMDI

The equation of motion developed herein considers a multi-degree of freedom 2D frame equipped with a TMDI as shown in Figure 2. For each level of the frame, the properties such as stiffness, damping, and mass are represented with the spring constant of stiffness k_i, the viscous damper with damping constant c_i, and a concentrated mass m_i, respectively, where i stands for each level of the frame.

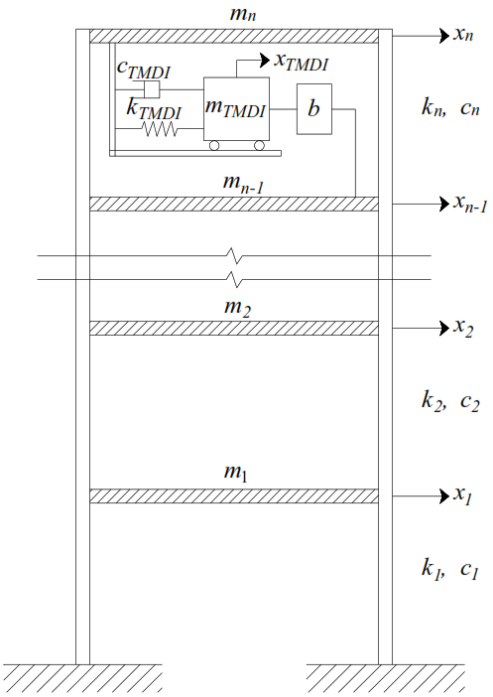

Figure 2: A *n* degrees of freedom system equipped with a TMDI.

Note the TMDI located in the upper level of the frame resembles a traditional TMD with an added inerter connecting the TMD and level *n-1*. The properties that characterized the device are almost the same as those for each level of the frame, therefore the mass is represented by m_{TMDI} and the stiffness and damping of the device are k_{TMDI} and c_{TMDI}, respectively. The only new parameter implemented is the constant b which refers to the inertance of the TMDI, and it provides information about the device's ability to resist changes in its motion.

The motion for the frame of $n+1$ degrees of freedom specified above is described by equation (2) where $\ddot{\boldsymbol{x}}(t)$, $\dot{\boldsymbol{x}}(t)$ and $\boldsymbol{x}(t)$ are the $n+1$ acceleration, velocity, and displacement vectors respectively and $\boldsymbol{F_{ext}}$ is the external force applied to the structure.

$$\boldsymbol{M}\ddot{\boldsymbol{x}}(t) + \boldsymbol{C}\dot{\boldsymbol{x}}(t) + \boldsymbol{K}\boldsymbol{x}(\boldsymbol{t}) = \boldsymbol{F_{ext}}(t) \tag{2}$$

In equation (2), ***M, C,*** and ***K*** represent the structure's mass, damping, and stiffness matrix, respectively of order *(n+1)* x *(n+1)* considering the degrees of freedom of the structure itself and the control device. They can be calculated as follows:

$$\boldsymbol{M} = \begin{bmatrix} m_1 & 0 & 0 & 0 & \cdots & \cdots & 0 \\ 0 & m_2 & 0 & 0 & \ldots & \cdots & 0 \\ 0 & 0 & m_3 & 0 & \cdots & \cdots & 0 \\ \vdots & \vdots & \vdots & \ddots & \cdots & \cdots & \vdots \\ \vdots & \vdots & \vdots & \vdots & m_{n-1}+b & 0 & -b \\ \vdots & \vdots & \vdots & \vdots & 0 & m_n & 0 \\ 0 & 0 & \cdots & \cdots & -b & 0 & m_{TMDI}+b \end{bmatrix} \tag{3}$$

$$\boldsymbol{C} = \begin{bmatrix} c_1+c_2 & -c_2 & 0 & 0 & \cdots & \cdots & 0 \\ -c_2 & c_2+c_3 & c_3 & 0 & \ldots & \cdots & 0 \\ 0 & c_3 & c_3+c_4 & c_4 & \cdots & \cdots & 0 \\ \vdots & \vdots & \vdots & \ddots & \cdots & \cdots & \vdots \\ \vdots & \vdots & \vdots & -c_{n-1} & c_{n-1}+c_n & -c_n & 0 \\ \vdots & \vdots & \vdots & 0 & -c_n & c_n+c_{TMDI} & -c_{TMDI} \\ 0 & 0 & \cdots & 0 & 0 & -c_{TMDI} & c_{TMDI} \end{bmatrix} \tag{4}$$

$$\boldsymbol{K} = \begin{bmatrix} k_1+k_2 & -k_2 & 0 & 0 & \cdots & \cdots & 0 \\ -k_2 & k_2+k_3 & -k_3 & 0 & \ldots & \cdots & 0 \\ 0 & -k_3 & k_3+k_4 & -k_4 & \cdots & \cdots & 0 \\ \vdots & \vdots & \vdots & \ddots & \cdots & \cdots & \vdots \\ \vdots & \vdots & \vdots & -k_{n-1} & k_{n-1}+k_n & -k_n & 0 \\ \vdots & \vdots & \vdots & 0 & -k_n & k_n+k_{TMDI} & -k_{TMDI} \\ 0 & 0 & \cdots & 0 & 0 & -k_{TMDI} & k_{TMDI} \end{bmatrix} \tag{5}$$

3 TMDI OPTIMIZATION

In order to design a properly functioning TMDI device, it is necessary to optimize the parameters that govern its performance. This optimization process involves finding the optimal values for the frequency and damping ratio of the device, which will ensure that it is able to effectively reduce the structural response of the building to wind.

3.1 Parameters that govern a TMDI

To design a TMDI it is necessary to define the parameters that are going to govern the device and therefore need to be optimized to mitigate the displacements and accelerations experienced by the structure. In equations (6) and (7) the critical damping ratio, ξ_{TMDI} and frequency ratio, ν_{TMDI} are described where m_{TMDI}, c_{TMDI}, k_{TMDI}, and b are the properties of the TMDI defined in the mathematical model and ω_1 is the fundamental frequency of the structure.

$$\nu_{TMDI} = \frac{\omega_{TMDI}}{\omega_1} = \frac{\sqrt{\dfrac{k_{TMDI}}{m_{TMDI}+b}}}{\omega_1} \tag{6}$$

$$\xi_{TMDI} = \frac{c_{TMDI}}{2(m_{TMDI}+b)\omega_{TMDI}} \tag{7}$$

In addition to the natural frequency and critical damping ratio, there are two other parameters that define the TMDI. They are not intended to be optimized but kept constant throughout the process. They are the device mass ratio, μ, and the inertance ratio, β, defined in equations (8) and (9), respectively, where Ms represents the total mass of the structure.

$$\beta = \frac{b}{Ms} \tag{8}$$

$$\mu = \frac{m_{TMDI}}{Ms} \tag{9}$$

As the optimization problem involves two parameters, it is considered a two-dimensional problem, and it is necessary to establish the limits within which the optimal values can be found. This is done by defining the range of possible values for each of the parameters to be optimized that has been further investigated [27–30].

$$0.00 \leq \zeta_{\text{TMDI}} \leq 0.50 \tag{10}$$

$$0.50 \leq \nu \leq 2.00 \tag{11}$$

To find the optimal parameters for the TMDI device, it is essential to define the objective functions that the optimization algorithm will work on. These objective functions are used to evaluate the performance of the device and determine how well it is able to reduce the structural response of the building. The optimization algorithm then searches through different combinations of parameter values to find the combination that results in the best performance as defined by the objective functions.

In this particular case of study, the objective functions are defined as the minimization of the maximum peak displacement ($x_{i\,peak}$) and minimizing the root mean square (RMS) value of acceleration ($RMS(\ddot{x}_i)$) of the structure as shown in equations (12) and (13), respectively.

$$J_1 = \min\left(max\left(\left|x_{i\,peak}\right|\right)\right) \tag{12}$$

$$J_2 = \min\left(max\left(\left|RMS(\ddot{x}_i)\right|\right)\right) \tag{13}$$

3.2 Grey wolf optimizer (GWO) algorithm

The Grey Wolf Optimizer algorithm is a swarm intelligence method proposed by Mirjalili *et al.* [24] and was inspired by the hunting behavior of grey wolves. It is a nature-inspired metaheuristic algorithm used to optimize solutions for a problem by mimicking the hierarchy and cooperation of a pack of grey wolves when hunting for prey. GWO is a simple, fast, and efficient optimization algorithm that has been applied to a wide range of optimization problems. It has been shown to be a powerful tool for solving complex optimization problems. The wolf that has the most optimal

solution is the alpha (α), and the one with the second and third best solution is the beta (β) and delta (δ), respectively. Other candidate solutions are omega (ω). The advantage of the algorithm over others is that omegas keep searching and updating its position depending on the best solution found. The optimization process can be described as follows [24, 31] :

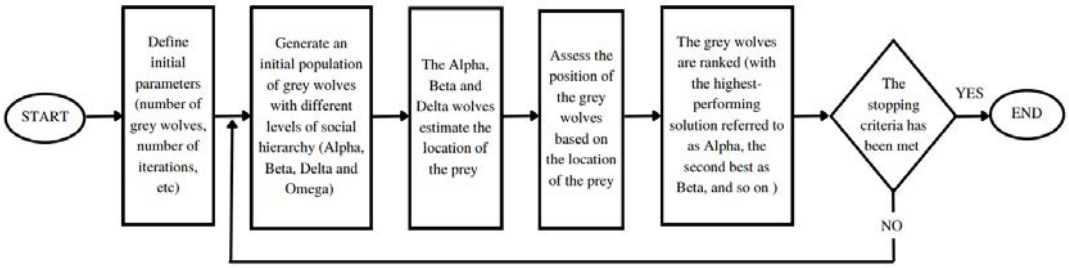

Figure 3: Grey wolf flowchart.

4 WIND LOAD

To analyze the dynamic wind load, the procedure proposed by Franco [32] will be applied. The approach consists of transforming the power spectrum of wind into fluctuating pressures represented by a number of harmonic functions. The procedure proposed by Franco provides an efficient and reliable method to generate the dynamic wind load, considering the different modes of vibration of the structure [33].

Important data such as the location and the topographic characteristics of where the structure of interest is located, need to be considered to find the basic parameters of wind speed. For the case of study in this paper, the Colombian earthquake-resistant design code, Normas Colombianas de Diseño y Construcción Sismoresistente NSR-10 [34], will be applicable due to the location of the building analyzed.

Figure 4 and Figure 5 demonstrate the results of the wind load analysis for the building. Figure 4 shows the fluctuating pressure of the wind over time, while Figure 5 illustrates the wind load acting on the 37th level. These results were obtained by using the methodology described above to simulate a dynamic wind load. These figures provide important information about the wind loads that the building will be subjected to and will be used to evaluate the structural response of the building and to determine the effectiveness of different control strategies.

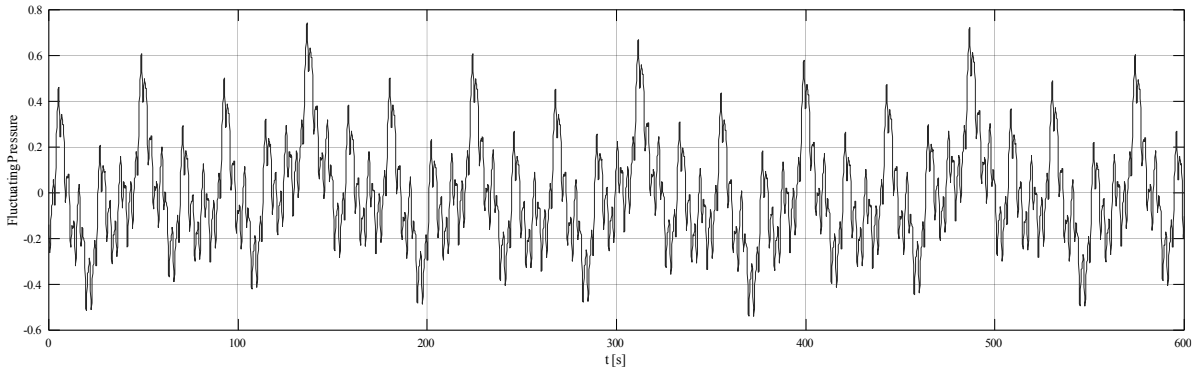

Figure 4: Fluctuating pressures of the wind.

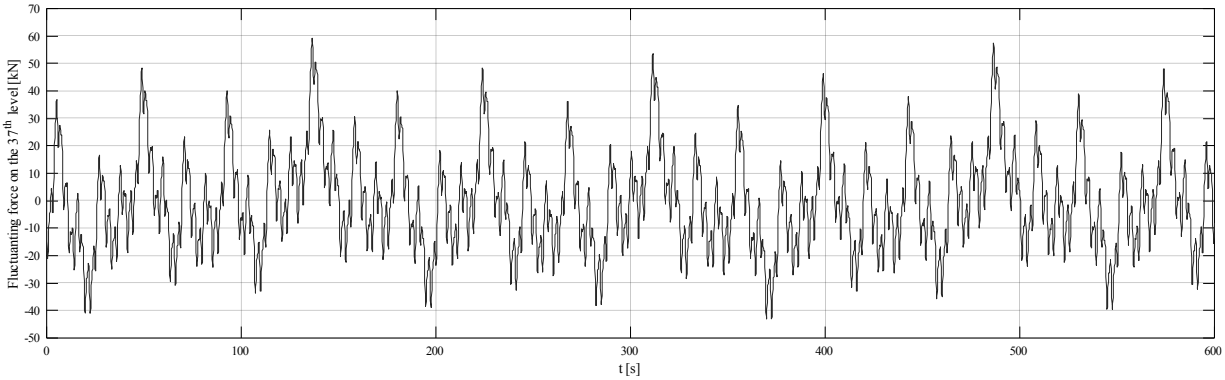

Figure 5: Wind load in the 37th level through time.

5 CASE OF STUDY

The mathematical model of a TMDI-controlled system is implemented in a real structure modeled as a plane frame, to evaluate its performance when it is subjected to wind load. The structure that was modeled and used in this case of study is *Cantagirone Tre Piú,* a residential building located in Medellín, Colombia. This building has 37 levels, with a height of 3.9 m per level. The total height is 144 m above ground level and the structure is 38 m wide where the modeled frame is. The building has a structural system that consists of reinforce concrete resisting frames alongside structural walls in the corners to improve the stiffness of the building. In Figure 6 the typical plan view and elevation of the building are shown.

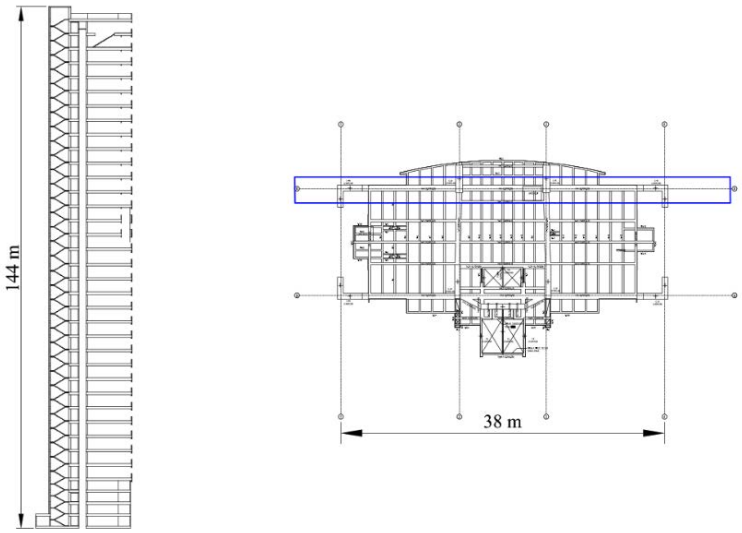

Figure 6: Elevation and plan view of *Cantagirone Tre Piú* building.

The analysis was made by reducing the plane frame to a single degree of freedom per level. To achieve this, a rigid floor diaphragm was assumed to obtain one degree of freedom for all horizontal translational nodes per level. Also, the columns were assumed axially infinitely rigid to eliminate all vertical translational degrees of freedom. Lastly, the rotational degrees of freedom were expressed in terms of the remaining horizontal translational degrees using static condensation. After

these assumptions the matrices of mass and stiffness of order *37* x *37* could be found. The damping matrix was determined by applying the Rayleigh method, using a structural damping value of 5% in the first and last modes of vibration. In Table 1, the result of the modal analysis performed in the structure is presented for the first six modes.

Mode	T [s]	F [Hz]	ω [rad/s]
1	0.8705	0.1828	1.1488
2	0.2614	0.6088	3.8254
3	0.1317	1.2083	7.5917
4	0.0801	1.9869	12.4838
5	0.0535	2.9722	18.6752
6	0.0385	4.1385	26.0030

Table 1: Modal properties of the plane frame.

6 RESULTS

The results obtained from the controlled response are categorized into two groups: the response of the controlled structure with the aim of reducing the highest peak displacement, represented by objective function J_1; and the controlled structural response with the objective of minimizing the RMS value of acceleration, represented by objective function J_2.

6.1 Algorithm Calibration

To calculate the controlled response, a calibration process was carried out in which the best combination of search inputs was sought so that the algorithm would search for the optimal parameters for the TMDI. The final selections for the optimization process resulted in 100 wolves and 20 iterations for the first objective function J_1 and 25 wolves with 10 iterations for the second objective function J_2. In order to select the wolf and iteration combinations that resulted in the best outcome, a trial-and-error process was carried out. Several combinations were tested to observe which one resulted in the maximum reduction while still optimizing time and computational efficiency. Through this process, an understanding of the problem was gained, which allowed decisions to be made regarding the selection of the best wolves and iteration combinations. Additionally, values were chosen to remain constant throughout the procedure, including the device mass ratio, μ, and the inertance ratio, β, both of which were fixed at 5% based on satisfactory results shown in previous research [16, 21].

6.2 Uncontrolled response

To have a better understanding of how the structure behaves under wind load, Table 2 summarizes the behavior of some levels in the building. It can be observed that the maximum displacement of each floor increases as the level increases, as does the acceleration. In both cases, the most critical value is on the last floor, where the peak displacement is 0.416 m, and the peak acceleration is 0.3047 m/s^2. This behavior is also reflected in the RMS values of displacement and acceleration, which are at their highest on the last floor reaching 0.1482 m and 0.1741 m/s^2 respectively. This trend is expected and demonstrates the importance of effectively controlling the response of the structure, especially at higher levels.

Level	Maximum uncontrolled displacement [m]	RMS value of uncontrolled displacement [m]	Maximum uncontrolled acceleration [m/s^2]	RMS value of uncontrolled acceleration [m/s^2]
1	0.0012	0.0004	0.0306	0.0005
5	0.0264	0.0092	0.0583	0.0103
10	0.1024	0.0361	0.0739	0.0414
15	0.1899	0.0675	0.1363	0.0782
20	0.2718	0.0972	0.1929	0.1131
25	0.3373	0.1211	0.2401	0.1412
30	0.3836	0.1380	0.2777	0.1616
35	0.4083	0.1470	0.3014	0.1727
37	0.4116	0.1482	0.3047	0.1741

Table 2: Uncontrolled response of the structure under wind load.

6.3 Controlled response

The response of the controlled structure can be viewed in Table **3**, when the objective function used during the optimization process was J_1. For this scenario, the parameters that govern the device were found to be 0.001 for the damping ratio and 0.995 for the frequency ratio.

Level	Maximum controlled displacement under J_1 [m]	RMS value of controlled displacement under J_1 [m]	Maximum controlled Acceleration under J_1 [m/s^2]	RMS value of controlled acceleration under J_1 [m/s^2]
1	0.0008	0.0003	0.0306	0.0002
5	0.0174	0.0056	0.0583	0.0030
10	0.0666	0.0215	0.0669	0.0120
15	0.1221	0.0393	0.0922	0.0228
20	0.1728	0.0557	0.1237	0.0317
25	0.2124	0.0687	0.1359	0.0384
30	0.2400	0.0780	0.1672	0.0448
35	0.2547	0.0831	0.1940	0.0495
37	0.2565	0.0839	0.2210	0.0502

Table 3: Controlled response of the structure under $\boldsymbol{J_1}$.

The displacement and acceleration of level 37th are displayed in Figure **7**.a and Figure **7**.b respectively. The RMS value of displacement and acceleration for each level is shown in Figure **7**.c and Figure **7**.d respectively. It can be noted that peak displacement on the top level had a reduction of 37.67% going from 0.4116 m to 0.2565 m after the device is implemented. In the case of acceleration, a reduction is also observed, with a decrease from 0.3047 m/s^2 to 0.2210 m/s^2, resulting in a reduction of 27.47%. In a similar manner to the behavior of peak displacement and acceleration, the value of the RMS for both displacement and acceleration experiences a reduction of 43.40% and 71.17%, respectively.

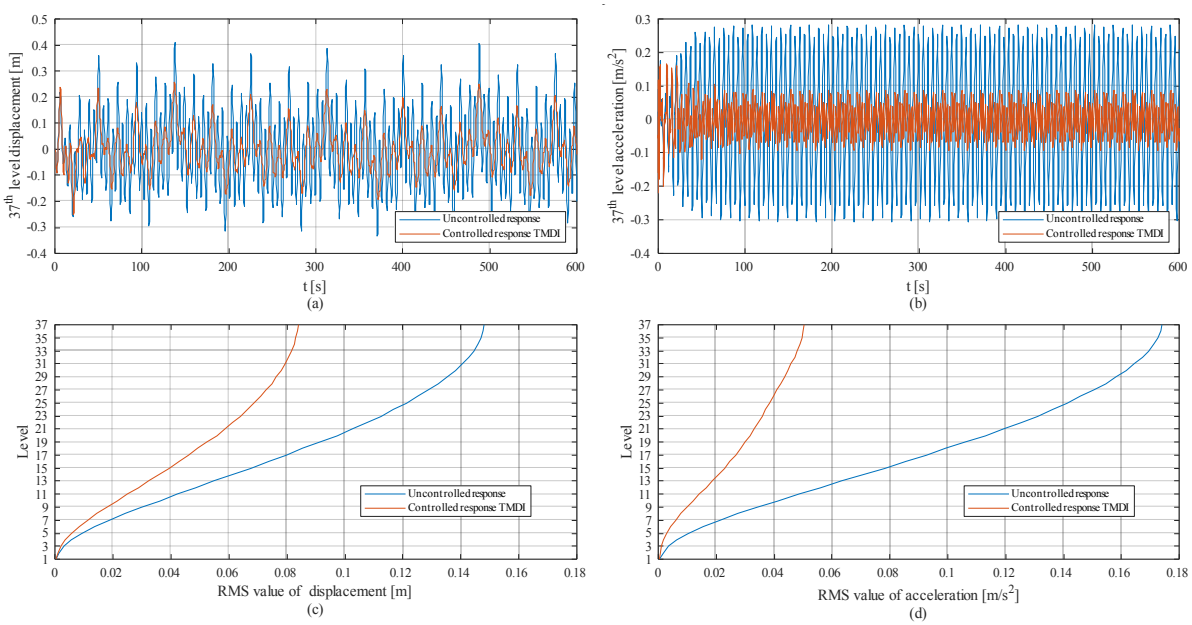

Figure 7. Structural controlled response using J_1. (a) Uncontrolled and controlled displacements on the 37th level. (b) Uncontrolled and controlled accelerations on the 37th level. (c) Uncontrolled and controlled RMS value of displacement. (d) Uncontrolled and controlled RMS value of acceleration.

In the optimization process, the second objective function tried was J_2, aimed to decrease the RMS value of acceleration. Satisfactory results were obtained and the controlled response at various levels of the structure can be seen in Table 4. This response was achieved once the design parameters of the device were found to be 0.01 for the damping ratio and 1.03 for the frequency ratio.

Level	Maximum controlled displacement under J_2 [m]	RMS value of controlled displacement under J_2 [m]	Maximum controlled Acceleration under J_2 [m/s^2]	RMS value of controlled acceleration under J_2 [m/s^2]
1	0.0008	0.0003	0.0306	0.0002
5	0.0167	0.0057	0.0583	0.0031
10	0.0641	0.0217	0.0669	0.0127
15	0.1199	0.0399	0.0921	0.0244
20	0.1732	0.0567	0.1232	0.0346
25	0.2171	0.0701	0.1476	0.0428
30	0.2498	0.0799	0.1682	0.0504
35	0.2687	0.0854	0.1950	0.0559
37	0.2718	0.0862	0.2209	0.0568

Table 4: Controlled response of the structure under J_2.

Figure 8 displays the controlled response of the building when J_2 was used. Figure 8.a and Figure 8.b shows the controlled displacements and accelerations respectively alongside the uncontrolled

response for comparison purposes. Similarly, Figure 8.c and Figure 8.d show the RMS value of displacement and acceleration respectively. The displacement has reduced from 0.4116 m to 0.2718 m, exhibiting a reduction of 33.95%. For the case of the acceleration, the value decreased from 0.3047 m/s^2 to 0.2209 m/s^2, resulting in a reduction of 27.51%. Finally, the reductions experienced by the RMS value of displacement and acceleration were of 41.80% and 67.36%, respectively.

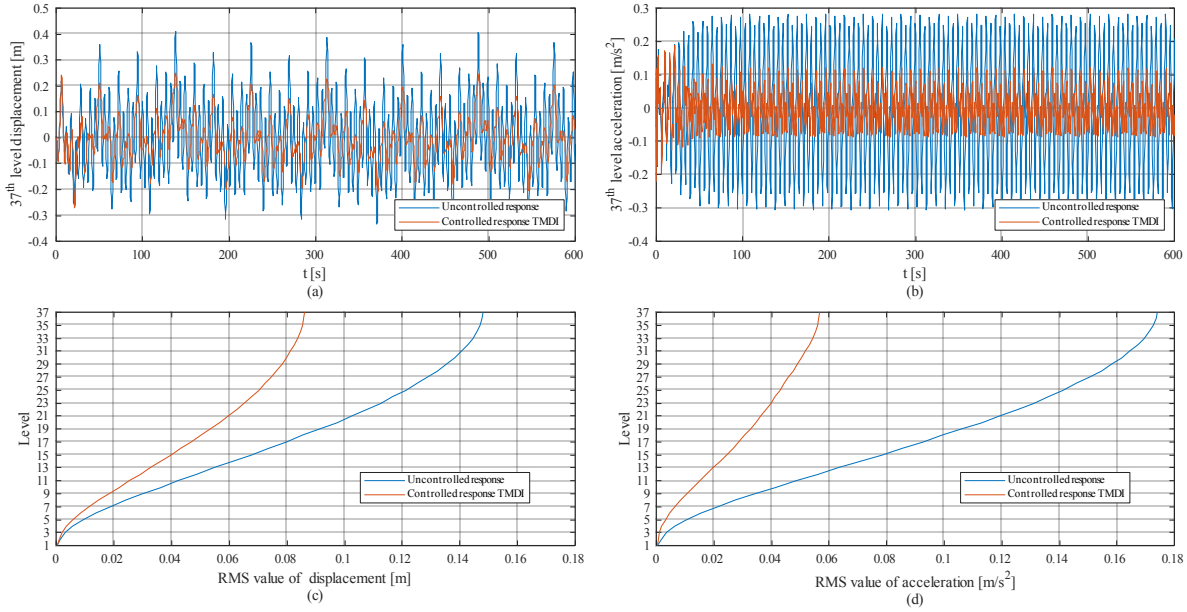

Figure 8. Structural controlled response using J_2. (a) Uncontrolled and controlled displacements on the 37th level. (b) Uncontrolled and controlled accelerations on the 37th level. (c) Uncontrolled and controlled RMS value of displacement. (d) Uncontrolled and controlled RMS value of acceleration.

7 CONCLUSIONS

- The optimization process carried out in this study involved searching for the optimal variables of the GWO that could identify the TMDI parameters resulting in the highest possible controlled response reduction. To accomplish this, the process was tried multiple times with various input variables to select the optimal combination. The selection criteria for identifying the best option were not solely based on achieving the maximum reduction but also on ensuring efficient use of computational resources. These findings highlight the importance of optimizing both computational resources and system performance in order to achieve the best results.

- Despite obtaining similar results with both objective functions, the response obtained was better when the objective function used for optimization was to reduce peak displacement. This may be because the response of a dynamic system subjected to wind load starts with calculating displacements, so when these are the target to be manipulated, the process is more direct and better results are obtained. In the case of the objective function that aimed to reduce the RMS of the acceleration, it can be said that it works in a similar way, since reducing the RMS requires decreasing some peaks and thereby achieving a more uniform response.

- The optimization resulting from the use of the objective function J_1 is governed by the following parameters, 0.001 for the damping ratio, and 0.995 for the frequency ratio. It can be observed that the value of the damping ratio is close to zero, indicating that the device requires a very small damper since the most influential factor in reducing the response is the inertial force generated by the inerter. This finding can provide insight into how to optimize the system for better performance, as a smaller damper can lead to reduced costs and greater efficiency.

- For this case of study, the TMDI system works optimally when the damping ratio is small. This finding is consistent with the understanding that the inerter provides a significant contribution to the reduction of dynamic response, and that the damping plays a less critical role in this process. However, it is important to note that the specific values for damping ratio that are considered small or optimal may depend on the specific characteristics of the structure and the loads it is subjected to.

REFERENCES

[1] B. F. Spencer Jr Nathan M Newmark Professor and S. Nagarajaiah Associate Professor, "State of the Art of Structural Control."

[2] Y. M. Parulekar and G. R. Reddy, "passive response control systems for seismic response reduction: a state-of-the-art review," 2009. [Online]. Available: www.worldscientific.com

[3] T. E. Saaed, G. Nikolakopoulos, J. E. Jonasson, and H. Hedlund, "A state-of-the-art review of structural control systems," *JVC/Journal of Vibration and Control*, vol. 21, no. 5. SAGE Publications Inc., pp. 919–937, Apr. 15, 2015. doi: 10.1177/1077546313478294.

[4] S. Masoud, S. Alehashem, A. Keyhani, and H. Pourmohammad, "Behavior and Performance of Structures Equipped With ADAS & TADAS Dampers (a Comparison with Conventional Structures)," 2008. [Online]. Available: https://www.researchgate.net/publication/311641178

[5] F. Mazza and A. Vulcano, "Control of the earthquake and wind dynamic response of steel-framed buildings by using additional braces and/or viscoelastic dampers," *Earthq Eng Struct Dyn*, vol. 40, no. 2, pp. 155–174, 2011, doi: 10.1002/eqe.1012.

[6] Y. Bigdeli and D. Kim, "Damping effects of the passive control devices on structural vibration control: TMD, TLC and TLCD for varying total masses," *KSCE Journal of Civil Engineering*, vol. 20, no. 1, pp. 301–308, Jan. 2016, doi: 10.1007/s12205-015-0365-5.

[7] J. P. den Hartog, *Mechanical Vibrations*. New York: McGraw-Hill, 1956.

[8] B. G. W Housner *et al.*, "Structural control: past, present, and future," 1997.

[9] A. Kaveh *et al.*, "Optimum parameters of tuned mass dampers for seismic applications using charged system search," 2015. [Online]. Available: https://www.researchgate.net/publication/273115251

[10] C. L. Lee, Y. T. Chen, L. L. Chung, and Y. P. Wang, "Optimal design theories and applications of tuned mass dampers," *Eng Struct*, vol. 28, no. 1, pp. 43–53, Jan. 2006, doi: 10.1016/j.engstruct.2005.06.023.

[11] A. Kaveh, M. Fahimi Farzam, H. Hojat Jalali, and R. Maroofiazar, "Robust optimum design of a tuned mass damper inerter," *Acta Mech*, vol. 231, no. 9, pp. 3871–3896, Sep. 2020, doi: 10.1007/s00707-020-02720-9.

[12] L. Marian and A. Giaralis, "Optimal design of a novel tuned mass-damper-inerter (TMDI) passive vibration control configuration for stochastically support-excited structural systems," *Probabilistic Engineering Mechanics*, vol. 38, pp. 156–164, Oct. 2014, doi: 10.1016/j.probengmech.2014.03.007.

[13] M. C. Smith, "Synthesis of mechanical networks: The inerter," *IEEE Trans Automat Contr*, vol. 47, no. 10, pp. 1648–1662, Oct. 2002, doi: 10.1109/TAC.2002.803532.

[14] A. Giaralis and A. A. Taflanidis, "Optimal tuned mass-damper-inerter (TMDI) design for seismically excited MDOF structures with model uncertainties based on reliability criteria," *Struct Control Health Monit*, vol. 25, no. 2, Feb. 2018, doi: 10.1002/stc.2082.

[15] A. Giaralis and L. Marian, "Use of inerter devices for weight reduction of tuned mass-dampers for seismic protection of multi-story building: the Tuned Mass-Damper-Interter (TMDI)," in *Active and Passive Smart Structures and Integrated Systems 2016*, Apr. 2016, vol. 9799, p. 97991G. doi: 10.1117/12.2219324.

[16] L. A. Lara-Valencia, Y. Farbiarz-Farbiarz, and Y. Valencia-González, "Design of a Tuned Mass Damper Inerter (TMDI) Based on an Exhaustive Search Optimization for Structural Control of Buildings under Seismic Excitations," *Shock and Vibration*, vol. 2020, 2020, doi: 10.1155/2020/8875268.

[17] A. Giaralis and F. Petrini, "Wind-Induced Vibration Mitigation in Tall Buildings Using the Tuned Mass-Damper-Inerter," *Journal of Structural Engineering*, vol. 143, no. 9, p. 04017127, Sep. 2017, doi: 10.1061/(asce)st.1943-541x.0001863.

[18] K. T. Tse, ; K C S Kwok, Y. Tamura, and M. Asce, "Performance and Cost Evaluation of a Smart Tuned Mass Damper for Suppressing Wind-Induced Lateral-Torsional Motion of Tall Structures," 2012, doi: 10.1061/(ASCE)ST.

[19] Z. Zhu, W. Lei, Q. Wang, N. Tiwari, and B. Hazra, "Study on wind-induced vibration control of linked high-rise buildings by using TMDI," *Journal of Wind Engineering and Industrial Aerodynamics*, vol. 205, Oct. 2020, doi: 10.1016/j.jweia.2020.104306.

[20] J. Dai, Z. D. Xu, and P. P. Gai, "Tuned mass-damper-inerter control of wind-induced vibration of flexible structures based on inerter location," *Eng Struct*, vol. 199, Nov. 2019, doi: 10.1016/j.engstruct.2019.109585.

[21] D. Caicedo, L. Lara-Valencia, J. Blandon, and C. Graciano, "Seismic response of high-rise buildings through metaheuristic-based optimization using tuned mass dampers and tuned mass dampers inerter," *Journal of Building Engineering*, vol. 34, Feb. 2021, doi: 10.1016/j.jobe.2020.101927.

[22] G. Bekdaş and S. M. Nigdeli, "Metaheuristic based optimization of tuned mass dampers under earthquake excitation by considering soil-structure interaction," *Soil Dynamics and Earthquake Engineering*, vol. 92, pp. 443–461, Jan. 2017, doi: 10.1016/j.soildyn.2016.10.019.

[23] M. Abdel-Basset, L. Abdel-Fatah, and A. K. Sangaiah, "Metaheuristic algorithms: A comprehensive review," in *Computational Intelligence for Multimedia Big Data on the Cloud with Engineering Applications*, Elsevier, 2018, pp. 185–231. doi: 10.1016/B978-0-12-813314-9.00010-4.

[24] S. Mirjalili, S. M. Mirjalili, and A. Lewis, "Grey Wolf Optimizer," *Advances in Engineering Software*, vol. 69, pp. 46–61, 2014, doi: 10.1016/j.advengsoft.2013.12.007.

[25] M. Panda and B. Das, "Grey Wolf Optimizer and Its Applications: A Survey," in *Lecture Notes in Electrical Engineering*, 2019, vol. 556, pp. 179–194. doi: 10.1007/978-981-13-7091-5_17.

[26] W. Fu-Cheng, C. Cheng-Wei, L. Min-Kai, and H. Min-Feng, "Performance Analyses of Building Suspension Control with Inerters," 2007.

[27] G. Bekdaş and S. M. Nigdeli, "Metaheuristic based optimization of tuned mass dampers under earthquake excitation by considering soil-structure interaction," *Soil Dynamics and Earthquake Engineering*, vol. 92, pp. 443–461, Jan. 2017, doi: 10.1016/j.soildyn.2016.10.019.

[28] J. Salvi and E. Rizzi, "Optimum tuning of tuned mass dampers for frame structures under earthquake excitation," *Struct Control Health Monit*, vol. 22, no. 4, pp. 707–725, Apr. 2015, doi: 10.1002/stc.1710.

[29] F. Petrini, A. Giaralis, and Z. Wang, "Optimal tuned mass-damper-inerter (TMDI) design in wind-excited tall buildings for occupants' comfort serviceability performance and energy harvesting," *Eng Struct*, vol. 204, Feb. 2020, doi: 10.1016/j.engstruct.2019.109904.

[30] D. De Domenico and G. Ricciardi, "An enhanced base isolation system equipped with optimal tuned mass damper inerter (TMDI)," *Earthq Eng Struct Dyn*, vol. 47, no. 5, pp. 1169–1192, Apr. 2018, doi: 10.1002/eqe.3011.

[31] H. Rezaei, O. Bozorg-Haddad, and X. Chu, "Grey wolf optimization (GWO) algorithm," in *Studies in Computational Intelligence*, vol. 720, Springer Verlag, 2018, pp. 81–91. doi: 10.1007/978-981-10-5221-7_9.

[32] M. Franco, "Direct Along-Wind Dynamic Analysis of Tall Structures," 1993.

[33] H. H. Barrios, N. M. Santacruz, and I. H. Ríos, "Respuesta eólica de estructuras tipo punto ante viento sintético," 2019.

[34] Ministerio de Ambiente Vivienda y Desarrollo Territorial, *Reglamento Colombiano de Construcción Sismo Resistente "NSR-10" Bogotá*. Asociación Colombiana de Ingeniería Sísmica: Bogotá, Colombia, 2010.